ADVANCES IN ATMOSPHERIC SCIENCES, VOL. 24, NO. 5, 2007, 833–844

ENSO Phase-Locking in an Ocean-Atmosphere Coupled Model FGCM-1.0

ZHENG Weipeng*[1,2] (郑伟鹏) and YU Yongqiang[1] (俞永强)

[1] *State Key Laboratory of Numerical Modeling for Atmospheric Sciences and Geophysical Fluid Dynamics, Institute of Atmospheric Physics, Chinese Academy of Sciences, Beijing* 100029

[2] *Graduate University of the Chinese Academy of Sciences, Beijing* 100049

(Received 6 September 2006; revised 11 December 2006)

ABSTRACT

The mean climatology and the basic characteristics of the ENSO cycle simulated by a coupled model FGCM-1.0 are investigated in this study. Although with some common model biases as in other directly coupled models, FGCM-1.0 is capable of producing the interannual variability of the tropical Pacific, such as the ENSO phenomenon. The mechanism of the ENSO events in the coupled model can be explained by "delayed oscillator" and "recharge-discharge" hypotheses. Compared to the observations, the simulated ENSO events show larger amplitude with two distinctive types of phase-locking: one with its peak phase-locked to boreal winter and the other to boreal summer. These two types of events have a similar frequency of occurrence, but since the second type of event is seldom observed, it may be related to the biases of the coupled model. Analysis show that the heat content anomalies originate from the central south Pacific in the type of events peaking in boreal summer, which can be attributed to a different background climatology from the normal events. The mechanisms of their evolutions are also discussed.

Key words: ENSO, phase-locking, coupled model

DOI: 10.1007/s00376-007-0833-z

1. Introduction

The El Niño-Southern Oscillation (ENSO) is the most prominent interannual variability in the tropical Pacific. Since the pioneering work of Bjerknes (1969), the understanding of ENSO has been greatly enhanced (see the special issue of *Journal of Geophysical Research*, Vol. 103, No. CC7, 1998). Studies have revealed that the growth of ENSO is due to the air-sea interactions in the tropical region and that its oscillation may be attributed to the equatorial heat content change through ocean dynamics (Bjerknes, 1969; Wyrtki, 1975, 1985; Zebiak and Cane, 1987). Many hypotheses have been put forward to address the mechanisms of ENSO (Neelin et al., 1998; Wang and Picaut, 2004), e.g., the delayed oscillator hypothesis (Suarez and Schophf, 1988; Battisti and Hirst, 1989), the recharge-discharge hypothesis (Jin, 1997), the western Pacific oscillator (Weisberg and Wang, 1997), the unified oscillator (Wang, 2001), and so on. Although these studies and hypotheses emphasized different aspects, most of them suggest heat content change of the western Pacific as the precursor of ENSO events. The heat content anomaly resulting from changes in the ocean surface wind field can be memorized in the thermocline and provides a delayed feedback mechanism, which may play an important role in the transition process of the whole coupled ocean-atmosphere system. The good relationship between thermocline depth and ENSO events is demonstrated by several studies (Li, 1997; Jin and An, 1999). From the ocean study results (NCEP ocean reanalysis: Wang et al., 1999), the heat content anomalies of the western Pacific have been shown to possess a wide meridional structure, and most are originated from the off-equatorial region. Therefore, the exchanges of equatorial and off-equatorial regions also have a significant impact on ENSO cycles.

Coupled climate models are very important tools for studying climate changes. Since the review of cou-

*Corresponding author: ZHENG Weipeng, zhengwp@mail.iap.ac.cn

pled models by Neelin et al. (1992), many new models with higher resolutions and more complicated parameterizations have come into practical use. Most of these models can reproduce the basic characteristics of the mean climatology and they are widely used in studies of global climate changes, as well as the climate system's responses to external forcing. To correctly simulate ENSO events is always an aim for coupled models. Some simple coupled models have been able to simulate ENSO-like phenomena (Zebiak and Cane, 1987; Suarez and Schophf, 1988) and clarify basic ENSO dynamics. Nevertheless, some important processes are omitted in these models. For example, a description of off-equatorial processes and remote effects are still incomplete and the mean climate state is prescribed artificially in these models. Thus we need more complicated and more comprehensive air-sea coupled model to help us better understand the air-sea interactions and the evolution of ENSO cycles. Over the past 20 years dramatic improvements have occurred in our ability to simulate ENSO and today's state-of-the-art coupled models show a clear improvement over previous generations in simulating tropical climatology (Mechoso et al., 1995; Delecluse et al., 1998; Covey et al., 2000; AchutaRao and Sperber, 2002, 2006; Guilyardi, 2006). Although these improvements are not sufficient for a totally realistic ENSO simulation, it provides an available model tool to study the tropical Pacific in more detail.

In this study, through comparing the coupled model's results with observations, the model's capability in simulating the basic mean climate is analyzed, and then further analysis of the model's ENSO variability is made in order to understand: (1) the origin and evolution of ENSO events in the coupled model, and (2) the relationship between ENSO variability and seasonal cycle change. The coupled model is described in section 2. Section 3 presents the mean climate of the FGCM-1.0 and compares them with observations. Section 4 discusses the evolution and possible mechanisms of two types of ENSO events in the FGCM-1.0. A summary follows in section 5.

2. Coupled model FGCM-1.0 and data

The coupled model used in this study is the Flexible General Circulation Model, version 1.0 (FGCM-1.0) (Yu et al., 2002; Yu et al., 2004; Yu and Liu, 2004 and Yu et al., 2007), which was developed at the State Key Laboratory of Numerical Modeling for Atmospheric Sciences and Geophysical Fluid Dynamics (LASG), Institute of Atmospheric Physics (IAP), China Academy of Science (CAS).

The atmospheric model component of FGCM-1.0

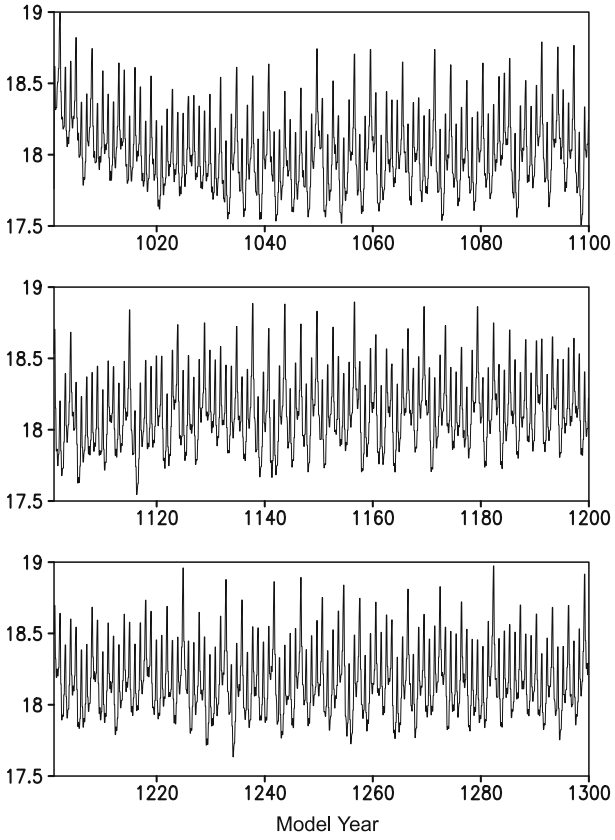

Fig. 1. Global mean SST of FGCM-1.0 (°C).

is the Community Atmosphere Model, version 2 (CAM2) (Collins et al., 2003), which was developed at NCAR based on CCM3, in which several parameterization schemes were implemented, such as the prognostic schemes of cloud water, the accumulation of cloud amount, more accurate long-wave radiation schemes for absorption and emission of water vapor, and a penetrative convection scheme. The vertical resolution of CAM2 was increased from 18 levels to 26 levels, while the horizontal resolution remained at T42, which is about $2.8° \times 2.8°$.

The oceanic model component of FGCM-1.0 is a LASG/IAP Climate system Ocean Model (LICOM) (Zhang et al., 2003; Liu et al., 2004). It is an updated version of a general ocean circulation model based on an OGCM developed by Jin et al. (1999). It covers from 75°S to 65°N (excluding the Arctic Ocean), and restoring boundary conditions are used for temperature and salinity at the northern and southern boundaries. The most significant modifications include: horizontal and vertical resolutions can be specified freely; and several options exist for the various physical parameterization schemes and parallel coding. In this study, the horizontal resolution of LICOM is subscribed to $0.5° \times 0.5°$, which means it is an eddy-

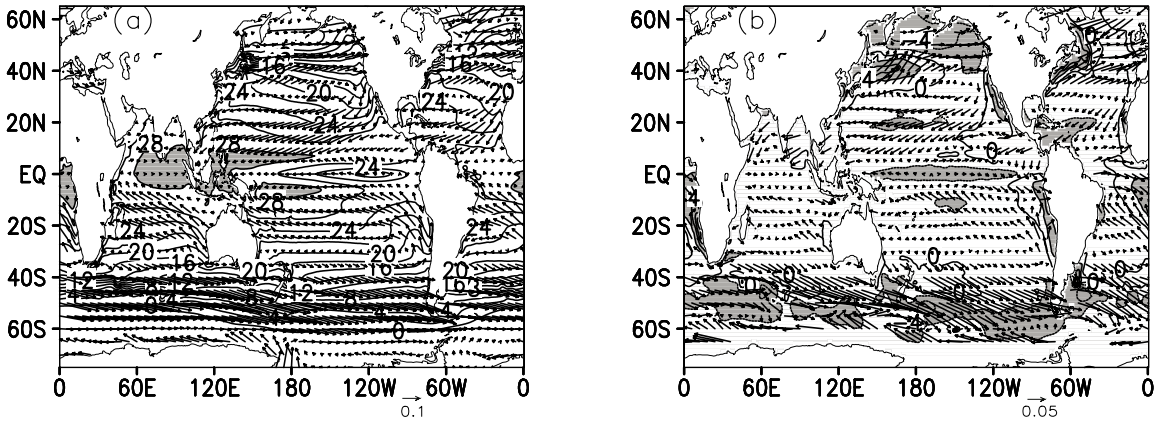

Fig. 2. Annual mean SST (°C) and wind stress vectors (N m^{-2}) for (a) FGCM-1.0 and (b) the difference between FGCM-1.0 and observations. Contour intervals are 2°C; SST greater than 28°C and those absolute values greater than 2°C are shaded.

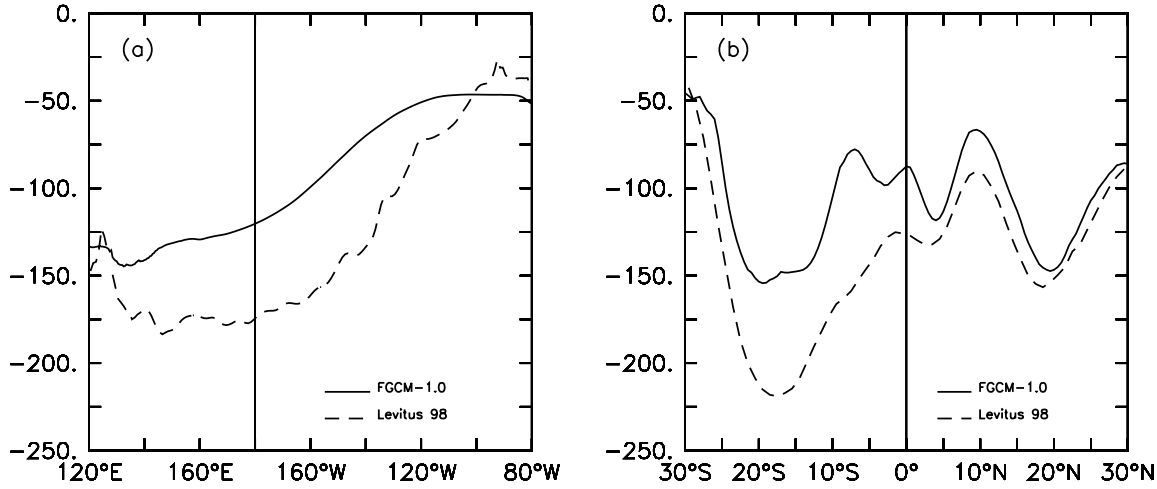

Fig. 3. Depth of thermocline (indicated by 20°C isothermal) for (a) along the equator (2°S–2°N averaged), and (b) meridional profile for the whole Pacific basin (120°E–80°W averaged). Solid lines are for FGCM-1.0, dash lines for Levitus 98.

permitting OGCM. Thirty levels are used in the vertical, with 12 equal levels in the upper 300 meters. With the high horizontal resolution, LICOM is capable of resolving the equator waveguide and the passage of Indonesian Throughflow (ITF).

CAM2 and LICOM are coupled through NCAR coupler version 5 (Kauffman and Large, 2002). A dynamic sea ice model—Community Sea Ice Model (CSIM) (Wetherly et al., 1998), and a land model-Community Land Model, version 2 (CLM2) (Bonan et al., 2002) are also coupled. FGCM-1.0 has been stably integrated for more than 300 years without a spin-up process or any flux adjustments. The simulation analyzed in this study is taken from the model year 101 to 190. The observation datasets used includes NCEP GODAS data (Kanamitsu et al., 2002) from 1979 to 2003, Levitus98 SST (Levitus et al., 1998), ERS wind stress etc.

3. Coupled model simulations

3.1 *Mean climate of the tropical Pacific*

The simulated global mean SST does not show any significant cooling or warming trend (Fig. 1). Because the model has no spin-up process in advance, the global mean SST falls rapidly at the beginning, but it comes to a stable state after the 50th model year.

The large-scale patterns of SST and wind stress are captured by the coupled model. A major bias occurs around the equator; the cold tongue penetrates far too west into the western Pacific, and the warm pool is thus divided into two parts (Fig. 2a). As the

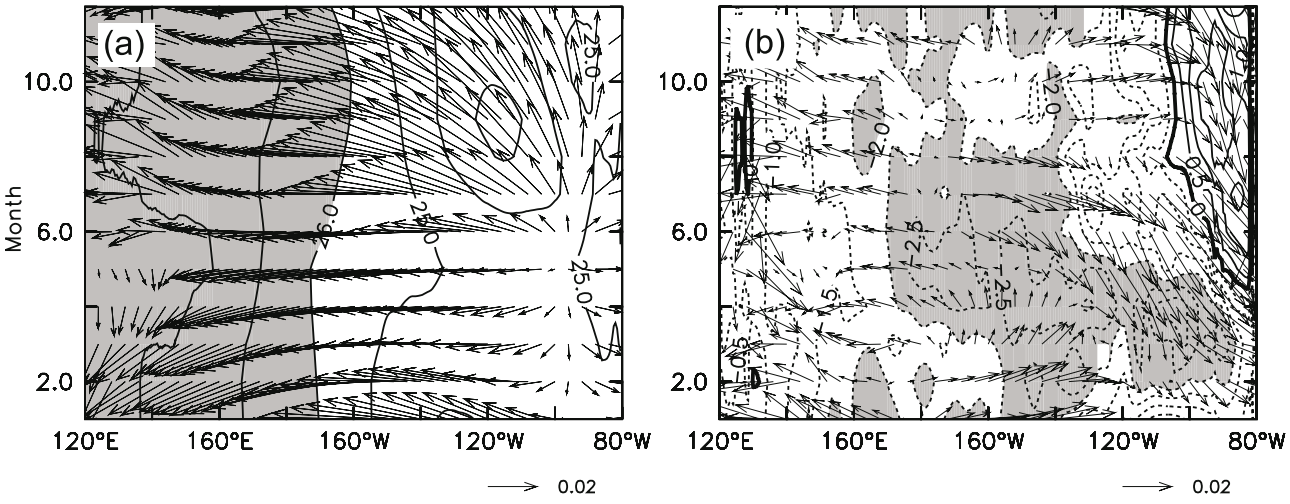

Fig. 4. Longitude-time cross section of SST (°C) and surface stress (N m^{-2}) averaged for 5°S–5°N. Zonal and meridional components of surface wind stress are shown as a wind vector; (b) the same as (a) except for the difference between model and observations.

model simulates larger than observed trade winds, the SSTs are slightly cooler in most parts of the ocean. The cooling centers in the northern Pacific and ACC (Antarctic Circumpolar Current) region are related to the stronger wind stress (Fig. 2b) and too much sea ice simulated in the model. Figure 2b also shows that the wind stresses over the eastern Pacific and along the western coast of Africa are weaker than the observations; therefore, upwellings in these regions are weakened and the SSTs are warmer than the observed. Warming centers are also found in the warm current regions (Kuroshio Current and Gulf Current), which may be related to the bias of the ocean model, such as insufficient poleward heat transport etc.

Figure 3 shows the model simulation of the thermocline, which is indicated by the 20°C isothermal. The depth of the 20°C isothermal is shallower than in the observations from the western Pacific to the Niño3 box, while it is deeper near the eastern Pacific coast (Fig. 3a). The diverging wind stress anomaly over the central Pacific (Fig. 2b) is responsible for the shallowing of the thermocline and the convergence to the eastern Pacific causes anomalous downwelling near the coast that deepens the thermocline there. In the observations, there exist two warm centers of heat content in the upper ocean of the tropical Pacific, which are located at the subtropical regions of each hemisphere. The tropical Pacific is a relatively cool area, with the minimum located between 5°–10°N where the ITCZ lies, which is due to the convergence of surface winds in this region; the Ekman pumping effect would cause strong upwelling that cools the upper sea water. The 20°C isothermal represents the heat content distribution as shown in Fig. 3b. The model captures some features of the thermocline pattern, but the depth of the 20°C isothermal is shallower across the subtropical and tropical regions mainly due to the stronger wind stress. What should be noted is that the model simulates the common bias of coupled models-a double ITCZ. The thermocline near 10°S is much shallower than in the observations, and thus the air-sea coupling is enhanced over the south Pacific in the model. This may have impacts on the evolution of ENSO events.

3.2 *Seasonal cycle*

To understand the behavior of the equatorial Pacific SST seasonal cycle between model and observations, Hovmöller diagrams of monthly mean SST and surface wind stress averaged for 5°S–5°N are displayed in Fig. 4. The model simulates a weaker SST annual cycle in the eastern Pacific, but the semiannual cycle in the western Pacific is not well reproduced (Fig. 4a). The model fails to simulate the gradual reduction of wind stress from the eastern to western Pacific. Compared with observations, the zonal wind stress is stronger in the western Pacific and weaker in the eastern part throughout the year. Horizontal wind divergence is found around the dateline in the western Pacific. Meridional wind in the eastern Pacific changes its sign between January–May and June–December. The northern wind component is much larger than the observed; therefore, weaker upwelling in the eastern Pacific leads to a warmer than observed SST in the latter half of the year (Fig. 4b). The SST is about 1–2°C cooler in the central Pacific and the maximum SST in the eastern Pacific during the spring season is missing

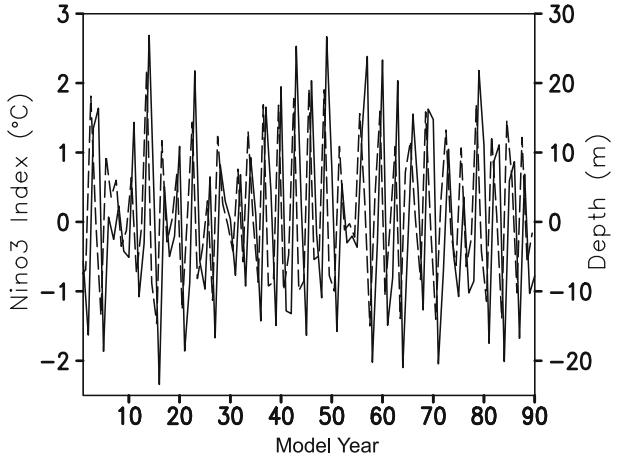

Fig. 5. Time series of the Niño-3 index (solid) and the variation of the 20°C isotherm (long dashed line) in the Niño-3 region.

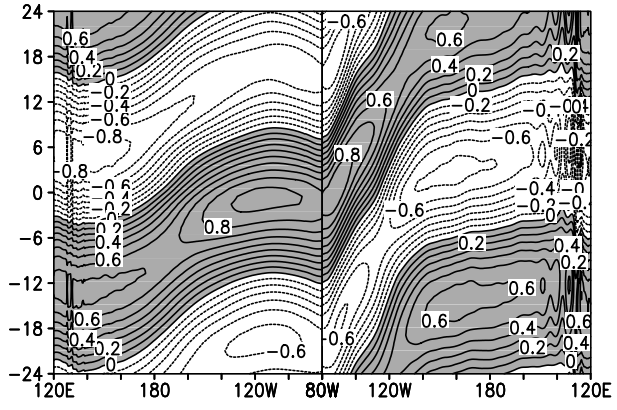

Fig. 6. Lag correlation of Niño-3 index and the heat content of the upper ocean: left, along the equator; right, 5°–8°N averaged.

in the model, which may be related to the anomalous upwelling caused by the cross equatorial wind.

3.3 *ENSO*

In this study, we adopt the SST anomaly (SSTA) of the Niño-3 region (5°S–5°N, 90°–150°W) as the index to analyze individual ENSO events. Figure 5 shows the time series of the model Niño-3 index. The standard deviation is about 1.5°C, which is nearly twice the observed. According to power spectrum analysis of the Niño-3 index, the model ENSO cycle has a period of about three years; it is reasonable that this period lies between two and seven years in the observations. This improvement of the model ENSO period may be related to the higher horizontal resolution. Figure 6 shows the lag correlation between the Niño-3 index and the upper ocean heat content (indicated by the ocean temperature of upper 300m). The propagation characteristics in the model can be explained by the delayed oscillator hypothesis (Suarez and Schophf, 1988; Battisti and Hirst, 1989); the anomaly starts from the subsurface of the western Pacific and propagates eastward along the thermocline in forms of Kelvin wave packages. When the anomaly reaches the eastern Pacific, it reflects and propagates westward along the off-equator region that forms an ENSO cycle. Figure 6 shows the model is also in agreement with the recharge-discharge hypothesis (Jin, 1997). The heat content leads the SST change by about six months in the Niño-3 box. Prior to El Niño, the heat content builds up gradually over the entire tropical Pacific (recharge) and during El Niño the accumulated warm water is flushed toward higher latitudes (discharge). After that, a negative heat content anomaly builds up in the equatorial Pacific and finally leads to a La Niña event.

An El Niño event with a SSTA larger than 1.5°C is defined as a strong event in this study. With this criterion, 21 strong El Niño and 20 strong La Niña events are identified in the time series of 90 model years. The composite analysis of strong El Niño events shows two types of El Niño phase-locking: one locked to boreal winter, with the warming starting from the previous November and reaching its peak during the next February, then terminating in August (Fig. 7a; Type I); and the other locked to boreal summer, where the warming starts from the previous September and peaks during July or August (Fig. 7b; Type II). Therefore, those 21 strong El Niño events can be further divided into 10 Type I and 11 Type II cases. Similar to the warm ENSO events, there are 9 Type I and 11 Type II cases in the total 20 strong La Niña events. Besides the time structure shifting by six months, the Type II events have weaker equatorial SST anomalies and the persistence of warming is also about four months shorter than Type I. The Type II El Niño event appears to be a model bias; as such a behavior is seldom seen in observations but is in other coupled models (Guilyardi et al., 2003). Since La Niña events develop in a similar way to El Niño, only with an opposite sign, the evolution and possible mechanisms of El Niño events is mainly discussed in the next section.

4. Mechanisms for ENSO phase change

4.1 *Type I El Niño event vs. 1997/98 observations*

The 1997/98 El Niño is the strongest event of recent years, and so a large amount of observations provide a pretty good benchmark to validate the model simulations. Figure 8 shows the time-longitude sections of equatorial anomalies of SST, zonal wind and

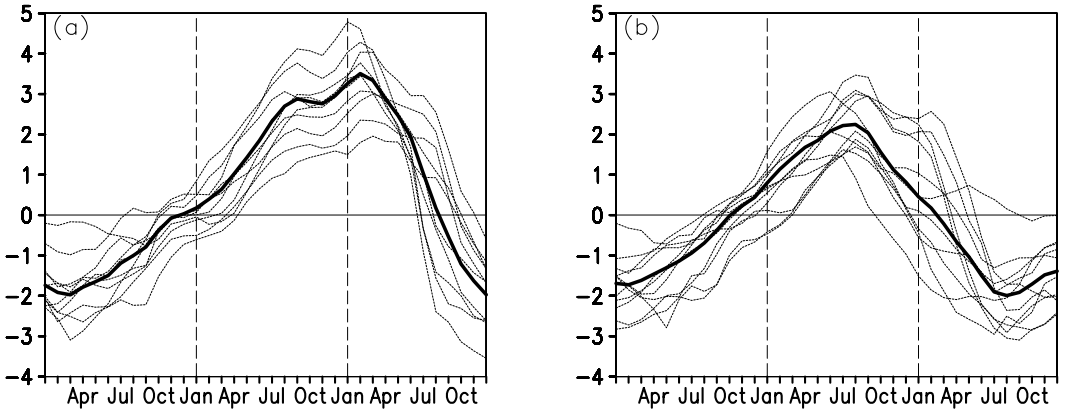

Fig. 7. The Niño-3 index of the composite of (a) Type I (10 cases) and (b) Type II (11cases). The solid black line is the average of all cases of each type (°C).

heat content. In 1996, the equatorial SST in the western Pacific was slightly warmer than usual (Fig. 8a) due to the strong easterlies (Fig. 8b). The heat content was also above normal (Fig. 8c). The warm anomalies crossed the basin in successive Kelvin waves in early 1997 and triggered the SST warming of the eastern Pacific (Fig. 8a). Due to SST-wind feedback described by Bjerknes (1969), the warming in the central and eastern Pacific was further amplified and reached a peak at the end of 1997. The westerly anomalies were characterized by the same eastward propagating characteristics as the migration of heat content anomalies. After the eastward migration of the positive heat content anomalies, the heat content of the western Pacific was reduced and turned to a negative state in mid 1997 (Fig. 8c). The negative anomalies began to propagate eastward in early 1998 and finally terminated the warming in the central to eastern Pacific. These equatorial phase changes have been described in great detail by McPhaden (1999).

The simulated Type I El Niño events, with the peak phase locked to boreal winter, resemble the observations well. The model composite shows many similar features to the observations both in the spatial pattern and time evolution (Figs. 8d–f). The heat content anomalies originate from the western Pacific and propagate eastward in forms of Kelvin waves, leading to the SST change of the central to eastern Pacific (Fig. 8d), while the westerly anomalies invade the central Pacific (Fig. 8e). Major differences are: when the El Niño event occurs, the whole tropical Pacific turns into a warmer state; the SST warming extends far too west into the western Pacific; the model fails to simulate the gradual eastward propagation of the surface wind stress seen in the observations; the easterly anomalies in the western Pacific are too weak or even replaced with westerly anomalies during the end of the warming year; and the corresponding heat content of the upper ocean is also weaker than in the observations.

Both in model simulations and the observations, the heat content anomalies appear to first originate in the northwestern Pacific (WNP) (figure not shown). Many studies—for example, Wang et al. (1999)—have suggested that evolution of the WNP heat content anomalies is a precondition of ENSO phase transition. What should be understood, then, is how the heat content anomalies accumulate in the WNP and in what way do the anomalies propagate to the equator waveguide. Two mechanisms have been proposed to explain the WNP heat content change:

(1) The accumulated effect of the off-equatorial free Rossby wave (Li, 1997),

(2) Local Ekman pumping caused by the local wind field (Weisberg and Wang, 1997; Wang et al., 1999).

Figure 9 shows the time evolution of the heat content anomalies and six-monthly integrals of wind stress curl averaged for 5°N and 15°N. Those two mechanisms mentioned above do play a role in both the observations and in the model. The westward propagation of heat content anomalies can only reach about 140°W, which implies the effect of off-equatorial free Rossby waves is relatively weak to the WNP, and within the longitude 120°E to 170°E the local wind forcing seems to play a more important role (Figs. 9a and 9c). During early 1997 (corresponding to the model warming year, Year 0), due to the positive wind stress curl, the upwelling of Ekman pumping contributes to the shallowing of the thermocline and decreases the heat content; the reverse mechanism can be found in the year 1996 (Year−1) and 1998 (Year +1), although the signals are weaker, especially in the observations (Figs. 9b and 9d).

Figure 10 presents the time evolution of the heat content anomalies zonally-averaged between 120°E

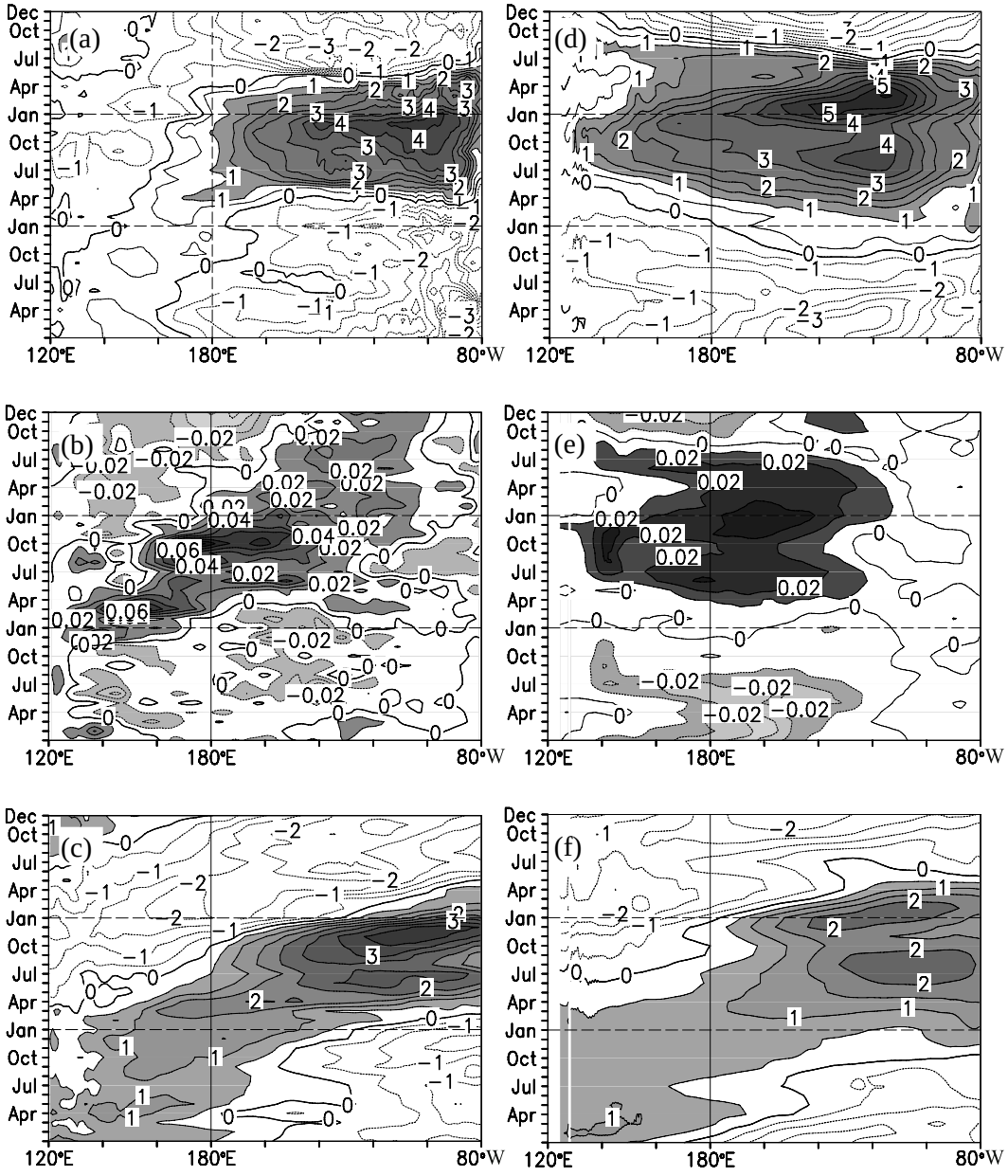

Fig. 8. The time-longitude evolution of the anomalies along the equator: (a) and (d) SST anomaly (°C); (b) and (e) Zonal wind (N m^{-2}); (c) and (f) Heat content of upper 300 m (°C); (a)–(c) is the observations of 1997/98 event in the GODAS dataset; (d)–(f) is the simulation of coupled model FGCM-1.0; vertical coordinate stands for the evolution time from Year −1 to Year +1.

and 170°E. The heat content anomalies originate in the off-equator region and propagate equatorward; they develop rapidly in the latter half of Year 0 (Fig. 10a). The six-month integral of wind stress curl is well correlated with the off-equatorial heat content anomalies, which further reveals the important role of local wind stress forcing. The change of the wind field is a response of the large-scale atmospheric circulation to the SST change, which is known as the Gill's response (Gill, 1980) and suggests a negative feedback for the ENSO turnabout. Near the end of Year 0, the heat content anomalies propagate equatorward into the equatorial waveguide and they are further transported to the central to eastern Pacific by Kelvin waves, which change the equatorial eastern Pacific, finally leading to the turnabout of the ENSO event.

As the ocean component model of FGCM-1.0 has a higher resolution, it can describe the ocean currents in more detail, especially the complex currents in the

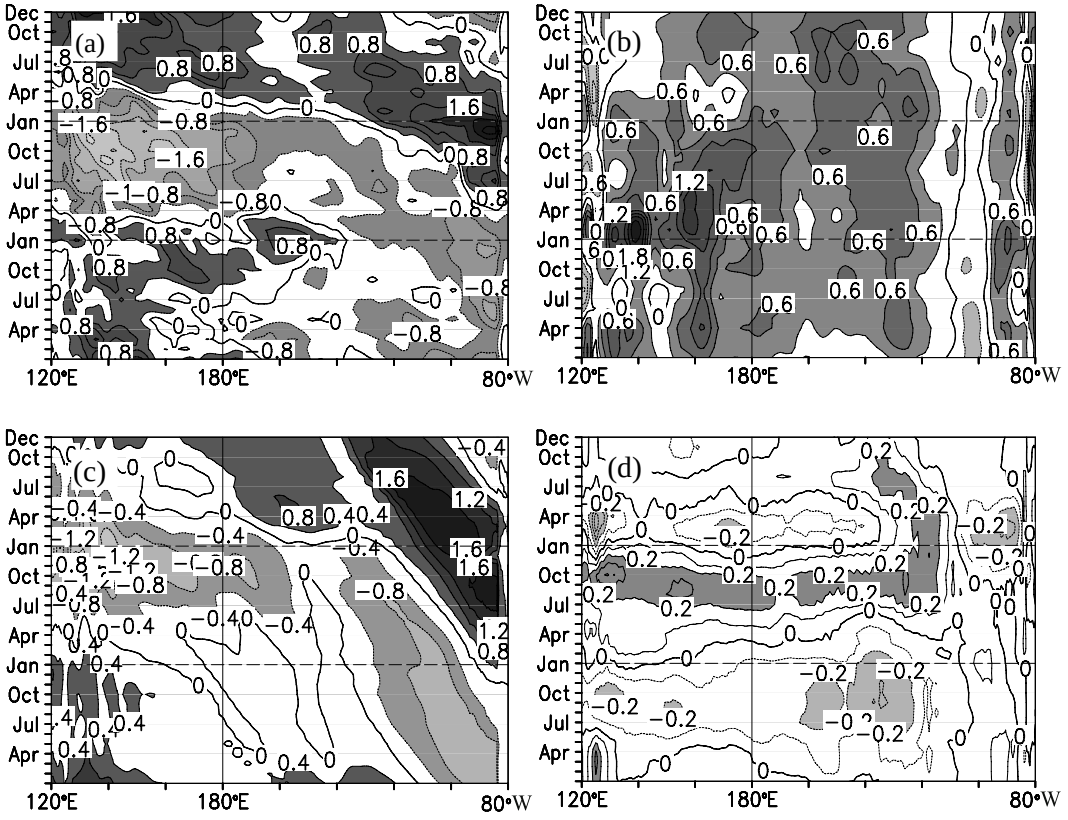

Fig. 9. The time-longitude evolution averaged between 5°N and 15°N: (a) and (c) Heat content (°C); (b) and (d) wind stress curl, integrated for six months. (a) and (b) are for the observations of 1997/98 El Niño in the GODAS dataset; (c) and (d) are the simulation of the coupled model FGCM-1.0.

tropical region. The analysis of oceanic currents suggests that the heat content anomalies are carried to the equatorial waveguide by complex northwestern Pacific currents. The anomalies are first advected to the west by the North Equatorial Current (NEC), and on reaching the western boundary, they are transported southward by the strong Mindanao Current. At about 5°N the anomalies veer to the east and they are advected by the NECC to the southeast and then merge with the Equatorial Under Current (EUC). Thus it completes the displacement of heat content anomalies from the northwest Pacific to the equatorial waveguide, which is an important component of the whole ENSO cycle.

4.2 *Type II El Niño event*

The coupled model simulates the second type of ENSO event with a peak during the boreal summer, which is seldom seen in observations. The only one special case is the 1993 spring warming of the eastern Pacific, which is generally called aborted El Niño, but it is not necessarily the same as Type II events in the coupled model. Besides the time of peak warming shifting by about six months, Type II events have a weaker SSTA and a shorter warming period when compared to Type I events (Fig. 11a). The heat content anomalies of Type II events also show a pattern of eastward propagation from the western Pacific (Fig. 11b). When considering the initiation of the anomalies, it was found that the anomalies appear first in the central south Pacific (Fig. 11c) and the role of the WNP is relatively weaker. The wind stress curl is well correlated to the heat content change, which further indicates the role of the local effect of the south Pacific (Fig. 11d).

The negative feedback mechanism of ENSO turnabout discussed for Type I also works for the Type II events. Major differences are the origin of the heat content anomaly and their evolutions after the summertime of the warming year (Year 0). The SSTA of Type I shows a small decrease after reaching the first warm peak and then increases again to reach the second maximum around February of the following year (Year +1), while the SSTA of Type II drops directly to a cold state (Fig. 7). It is proposed that this may be related to the model seasonal cycle and the bias of double

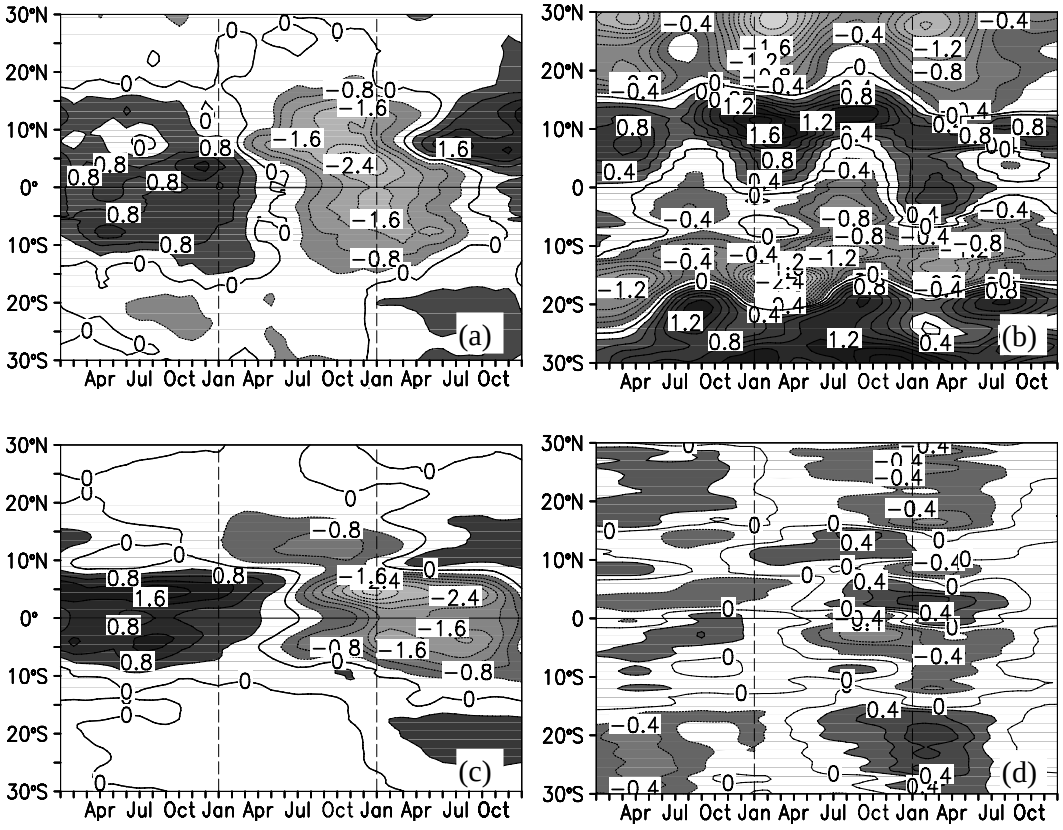

Fig. 10. The time-longitude evolution averaged between 120°E and 170°E: (a) and (c) heat content (°C); (b) and (d) wind stress curl, integrated for six months. (a) and (b) are for the observation of 1997/98 El Niño in GODAS dataset; (c) and (d) are the simulation for the coupled model FGCM-1.0.

ITCZ. Gill's response proposes that a warmer SSTA along the equator will lead to a cyclonic wind stress anomaly off the equator to the west of the warming region in both hemispheres. When the SST becomes warmer in the central to eastern Pacific, positive wind stress anomalies appear in the WNP and southwestern Pacific. However, the thermocline is much deeper in the south Pacific (Fig. 3b), the air-sea coupling strength is weaker than that in the WNP, and therefore we see that the negative feedback is more significant in the WNP and the heat content anomaly comes mostly from the WNP region. Yet in the coupled model, due to the double ITCZ, the thermocline shows a symmetric distribution about the equator. The thermocline in the south Pacific is much shallower when compared to the observations, which implies that the anomalous wind stress will play the equivalent role in the ENSO turnabout in the model simulations.

As for the Type II events, when the central to eastern Pacific becomes warmer around October of Year −1, negative wind stress curl occurs at the latitude of about 10°S, where the model simulates a shallower thermocline compared to the observations (Fig. 3b). Meanwhile, the Southern Pacific Convergence Zone (SPCZ) is strong and active, and the upwelling caused by the anomalous wind stress curl enhances the air-sea coupling strength; cooler water is pumped upward to reduce the SST and also the heat content in the following 4–6 months. Such feedback is also seen in the WNP, but it lags the south Pacific for about two months. What should be noted is that the seasonal cycle of the mean wind stress curl is larger than in the observations in the Southern Hemisphere, with the minimum located at 10°S of April and 6°S of August (figure not shown). Therefore, the combined effect of both the mean upwelling and anomalous upwelling will contribute to terminate the warming in the Niño-3 region in the middle of the warming year (Year 0). The displacement of the heat content from the south Pacific to the equatorial waveguide is associated with the Ekman drift driven by anomalous westerlies. Similar mechanisms have been raised to explain the heat content propagation of a coupled model (Guilyardi et al., 2003).

The impact of the south Pacific can also be found in Type I events. The Niño-3 SSTA shows a small

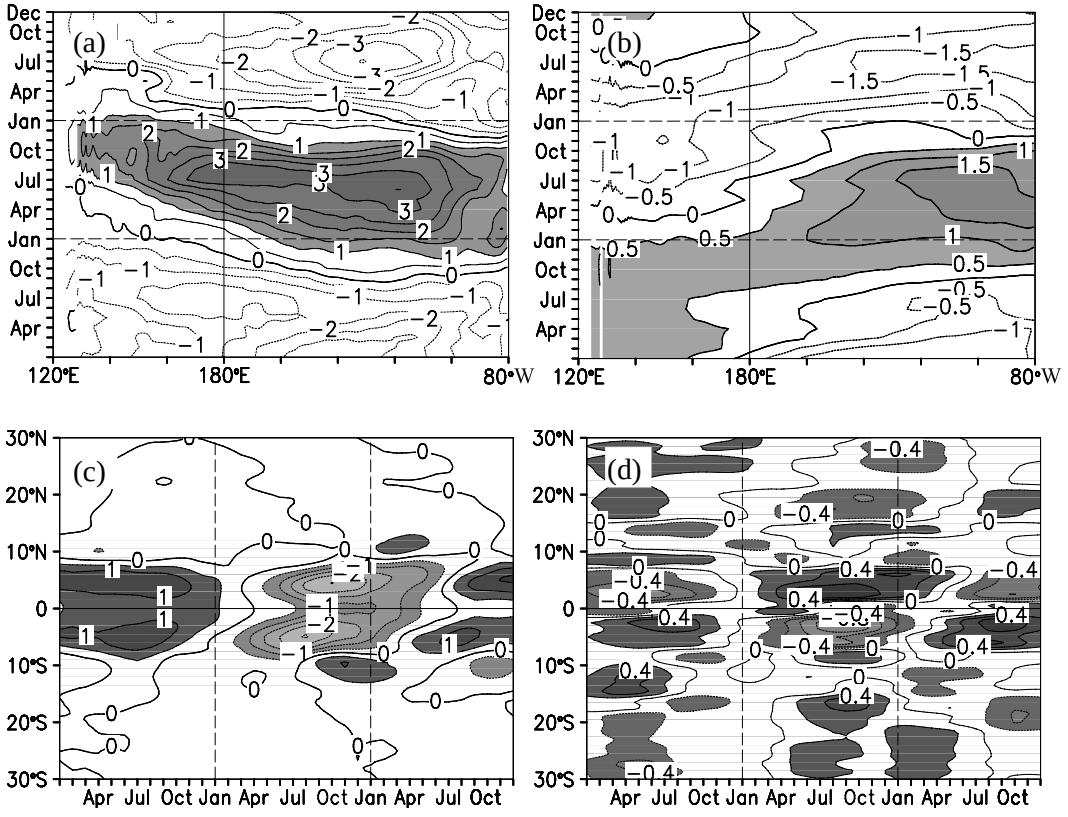

Fig. 11. The time-longitude evolution for Type II ENSO events in the coupled model FGCM-1.0: (a) SST anomaly (°C); (b) heat content along the equator; (c) heat content averaged between 140°E and 180°E; and (d) Wind stress curl integrated for six months, averaged between 140°E and 180°E.

decrease during the summertime of the warming year, and then increases again (Fig. 7a). Actually, it is still not known why the negative feedback cannot terminate the Type I events during the middle of the warming year. The composite analysis gives us some hints: the negative feedback seems to prefer to be stronger in the summer hemisphere when the atmospheric Gill's response is strongest; the anomalous wind stress curl in the south Pacific of Type I is weaker than Type II, which may be related to the large-scale climate pattern; and the displacement of the heat content anomaly are different between these two types of El Niño events. Further studies are needed to understand the differences.

5. Summary

In this study, the ability of a coupled model FGCM-1.0 to simulate the mean climatology was validated, and further discussion was presented regarding the possible mechanism of the phase-locking of ENSO events in the model. The coupled model successfully simulated the characteristics of the mean climatology and the interannual variability in the tropical Pacific without any flux corrections. The analysis of ENSO cycles suggested that this model supports the basic mechanisms proposed by various ENSO paradigms.

The coupled model FGCM-1.0 simulated a reasonable ENSO period of about three years, although it was too regular. Two types of phase-locking of ENSO events were found in the model: one with its mature phase locked to boreal winter and the other preferring to mature during the boreal summer. Such behavior of the Type II events was not frequently seen in the observations. Type I events resembled cases in the observations well, their space patterns and time evolutions both being similar to the strong 1997/98 case.

The northwestern Pacific (WNP; 5°–15°N, 120°–170°E) heat content anomalies were confirmed as the precondition to the ENSO phase change of the Type I events in the model. Ekman pumping caused by the local wind field plays a dominant role in the heat content change in the WNP region; if there are impacts of the free Rossby wave, it may play a secondary role. The phase change of both types of event in the model can be explained by a negative mechanism involving the ocean and atmosphere coupled system. For example, for Type I, as the SST rises in

the central to eastern Pacific, the atmospheric Gill's response generates an anomalous cyclonic circulation over the northwest Pacific, the anomalous wind stress curl causes upwelling in the ocean, and the effect lasts for several months and leads to a reduction in the local heat content. After the formation of the negative heat content anomalies, they are transported equatorward through a complex oceanic current system that eventually leads to SST cooling in the central to eastern Pacific. The displacement of the WNP heat anomalies is highly complicated, and with the higher resolution of the oceanic model LICOM, a possible path via the mean oceanic currents of the northwest Pacific is suggested. The anomalies can be effectively transported into the equatorial waveguide through advection of the mean currents, but other mechanisms, such as Ekman drift, should also be considered to be of some importance. Further studies are needed.

The Type II ENSO events whose phase is locked to boreal summer may be considered as a bias of the coupled model. A similar negative feedback mechanism also works for the phase transition of this type of event, but the differences lie in the initiation of the heat content anomalies and their propagation to the equatorial waveguide. The south Pacific plays a more important role in the evolution of Type II events. Since the coupled model simulated Southern Convergence Zone that was too strong and too zonal during the austral summer, the large-scale atmospheric circulation anomalies of the central-south Pacific may cause the heat anomalies to first occur in this region and the anomalous westerlies to drift an Ekman transport to the equator. The shallower thermocline in the south Pacific will enhance the air-sea coupling that further contributes to the negative mechanism of ENSO turnabout. Due to the shorter time of wind stress effect and the displacement to the equator, the SST anomalies do not fully develop and lead to a shorter warming period.

The successful simulation of ENSO features in many aspects by the coupled model FGCM-1.0 is encouraging, and thus it should be a useful tool to further investigate the mechanisms of tropical variabilities. A relationship between timing of El Niño onset and subsequent evolution has been discussed by Horri and Hanawa (2004), and some analysis of our model shows that the onset may have relationship with the phase-locking in a certain El Niño event. Analysis also shows that the model prefers to simulate a certain type of ENSO event under different background of climatology, and with a 300-year integration it is possible to discuss the decadal variability of ENSO. Much work still needs for further investigation.

Acknowledgements. We thank Prof. Xue-Hong Zhang of LASG, IAP, Prof. Bin Wang of the University of Hawaii and Prof. Fei-Fei Jin of Florida State University for their discussions. Thank the reviewers for the helpful suggestions. The computation of this study was carried out on the IBM SP690 of the Scientific Computation and Information Center in IAP, CAS. This study was jointly supported by National Natural Science Foundation of China grants (No. 40221503 and No. 40675049) and the CAS International Partnership Creative Group "The Climate System Model Development and Application Studies".

REFERENCES

AchutaRao, K., and K. R. Sperber, 2002: Simulation of the El Niño-Southern Oscillation: Results from the coupled model intercomparison project. *Climate Dyn.*, **19**, 191–209.

AchutaRao, K., and K. R. Sperber, 2006: ENSO simulation in coupled ocean-atmosphere models: Are the current models better? *Climate Dyn.*, **27**, 1–15.

Battisti, D. S., and A. C. Hirst, 1989: Interannual variability in the tropical atmosphere-ocean model: Influence of the basic state, ocean geometry and nonlineary. *J. Atmos. Sci.*, **45**, 1687–1712.

Bjerknes, J., 1969: Atmospheric teleconnections from the equatorial Pacific. *Mon. Wea. Rev.*, **97**, 163–172.

Bonan, G. B., K. W. Oleson, M. Vertenstein, and S. Levis, 2002: The land surface climatology of the Community Land Model coupled to the NCAR Community Climate Model. *J. Climate*, **15**, 3123–3149.

Collins, W. D., and Coauthors, 2003: Description of the NCAR Community Atmosphere Model (CAM2). National Center for Atmospheric Research, Boulder, Colorado, USA, 171pp.

Covey, C, and Coauthors, 2000: The seasonal cycle in coupled ocean-atmosphere general circulation models. *Climate Dyn.*, **16**, 775–787.

Delecluse, P., M. Davey, Y. Kitamura, S. Philander, M. Suarez, and L. Bengtsson, 1998: TOGA review paper: Coupled general circulation modeling of the tropical Pacific. *J. Geophys. Res.*, **103**, 14357–14373.

Gill, A. E., 1980: Some simple solution of heat-induced tropical circulation. *Quart. J. Roy. Meteor. Soc.*, **106**, 447–462.

Guilyardi, E., 2006: El Niño-mean state-seasonal cycle interactions in a multi-model ensemble. *Climate Dyn.*, **26**, 329–348.

Guilyardi, E., P. Delecluse, S. Gualdi, and A. Navarra, 2003: Mechanisms for ENSO phase change in a coupled GCM. *J. Climate*, **16**, 1141–1158.

Jin, F. F., 1997: An equatorial ocean recharge paradigm for ENSO. Part I: Conceptual model. *J. Atmos. Sci.*, **54**, 811–829.

Jin, F. F., and S.-I. An, 1999: Thermocline and zonal advective feedbacks within the equatorial ocean recharge oscillator model for ENSO. *Geophys. Res. Lett.*, **26**, 2989–2992.

Jin, X. Z., X. H. Zhang, and T. J. Zhou, 1999: Fundamental framework and experiments of the third generation of IAP/LASG world ocean general circulation model. *Adv. Atmos. Sci.*, **16**, 197–215.

Horri, T., and K. Hanawa, 2004: A relationship between timing of El Niño onset and subsequent evolution. *Geophys. Res. Lett.*, **31**, L06304, doi:10.1029/2003GL019239.

Kanamitsu, M., W. Ebisuzaki, J. Woollen, S.-K. Yang, J. J. Jnilo, M. Fiorino, and G. L. Potter, 2002: NCEP-DOE AMIP-II reanalysis (r-2). *Bull. Amer. Meteor. Soc.*, **83**, 1631–1643.

Kauffman, B. G., and W. G. Large, 2002: The CCSM Coupler Version 5.01: Combined User's Guide, Source Code Reference and Scientific Description. National Center for Atmospheric Research, Boulder, Colorado, USA, 46pp.

Levitus, S., and Coauthors, 1998: *NOAA Atlas NESDIS 18, WORLD OCEAN DATABASE 1998*. Vol. 1, US Government Printing Office, Washington D. C., USA, 346pp.

Li, T., 1997: Phase transition of the El Niño-Southern oscillation: A stationary SST mode. *J. Atmos. Sci.*, **54**, 2872–2887.

Liu, H. L., X. H. Zhang, W. Li, Y. Q. Yu, and R. C. Yu, 2004: An eddy-permitting Oceanic General Circulation Model and its preliminary evaluation. *Adv. Atmos. Sci.*, **21**(5), 675–690.

Mechoso, C. R., and Coauthors, 1995: The seasonal cycle over the tropical Pacific in coupled ocean-atmosphere general circulation models. *Mon. Wea. Rev.*, **123**, 2825–2838.

McPhaden, M., 1999: Genesis and evolution of the 1997–1998 El Niño. *Science*, **283**, 950–954.

Neelin, J. D., and Coauthors, 1992: Tropical air-sea interaction in general circulation models. *Climate Dyn.*, **7**, 73–104.

Neelin, J. D., D. Battisti, A. Hirst, F.-F. Jin, Y. Wakata, T. Yamagata, and S. Zebiak, 1998: ENSO theory. *J. Geophys. Res.*, **103**, 14261–14290.

Suarez, M. J., and P. S. Schophf, 1988: A delayed action oscillator for ENSO. *J. Atmos. Sci.*, **45**, 3283–3287.

Wang, B., R. Wu, and R. Lukas, 1999: Roles of the western North Pacific wind variation in thermocline adjustment and ENSO phase transition. *J. Meteor. Soc. Japan*, **77**, 1–16.

Wang, C., 2001: A unified oscillator model for the El Niño-Southern oscillation. *J. Climate*, **14**, 98–115.

Wang, C., and J. Picaut, 2004: Understanding ENSO physics–A review. *Earth's Climate: The Ocean—Atmosphere Interaction*, C. Wang et al., Eds., AGU Geophysical Monograph Series, No. 147, 21–48.

Weisberg, R. H., and C. Wang, 1997: A western Pacific oscillator paradigm for the El Niño-Southern Oscillation. *Geophys. Res. Lett.*, **24**, 779–782.

Wetherly, J. W., B. P. Briegleb, W. G. Large, and J. A. Maslanik, 1998: Sea ice and polar climate in the NCAR-CSM. *J. Climate*, **11**, 1472–1486.

Wyrtki, K., 1975: El Niño—The dynamic response of the equatorial Pacific Ocean to atmospheric forcing. *J. Phys. Oceanogr.*, **5**, 572–584.

Wyrtki, K., 1985: Water displacements in the Pacific and the genesis of El Niño cycles. *J. Geophys. Res.*, **90**, 7129–7132.

Yu, Y. Q., and X. Y. Liu, 2004: ENSO and Indian dipole mode in three coupled GCMs. *Acta Oceanologica Sinica*, **23**(4), 581–595.

Yu, Y. Q., R. C. Yu, X. H. Zhang, and H. L. Liu, 2002: A flexible coupled ocean-atmosphere general circulation model. *Adv. Atmos. Sci.*, **19**, 169–190.

Yu, Y. Q., X. H. Zhang, and Y. F. Guo, 2004: Global coupled ocean-atmosphere general circulation models in LASG/IAP. *Adv. Atmos. Sci.*, **21**, 444–455.

Yu, Y. Q., W. P. Zheng, H. L. Liu, and X. H. Zhang, 2007: The coupled climate model FGCM-1.0 in LASG. *Chinese Journal of Geophysics*. (in Chinese, in press)

Zebiak, S. E., and M. A. Cane, 1987: A model El Niño-Southern Oscillation. *Mon. Wea. Rev.*, **115**, 2262–2278.

Zhang, X. H., Y. Q. Yu, and H. L. Liu, 2003: The development and application of the Oceanic General Circulation Models Part I. The Global Oceanic General Circulation Models. *Chinese J. Atmos. Sci.*, **27**(4), 607–617.